Resistance of bismuth at low temperatures

V. S. Vinnik, I. Ya. Korenblit, E. A. Okhrem, and A. G. Samiŏlovich

B. P. Konstantinov Leningrad Institute of Nuclear Physics, Academy of Sciences of the USSR, Gatchina and Chernovtsy State University

A variational method is used to calculate the electrical resistivity tensors of electrons and holes in bismuth, governed by the scattering on phonons in the temperature range $0.1 \leq T \leq 8°$k. The electron constant-energy surface is approximated by three triaxial ellipsoids, whereas the hole surface is represented by an ellipsoid of revolution; according to Korenblit [Sov. Phys. Semicond. **2**, 1192 (1969)], the phonon spectrum is anisotropic. It is shown that the temperature dependence of the phonon electrical resistivity of electrons is linear at $T > 6°$k but obeys $\rho^T \propto T^5$ at $T < 0.15°$K. In the intermediate range $0.15 < T < 6°$K the temperature dependence of the resistivity is not described by a power law. In particular, it is shown that bismuth does not satisfy conditions under which the phonon resistivity would depend quadratically on temperature. The calculated temperature-dependent component of the resistivity is in good agreement with the experimental results of Uher and Pratt [Phys. Rev. Lett. **39**, 491 (1977)] in a wide range $0.15 < T < 4°$K.

PACS numbers: 72.10.Di, 72.15.Eb

INTRODUCTION

In spite of the fact that much work has been done on the transport phenomena in bismuth, it is still not clear which mechanism governs the temperature-dependent component of the resistivity ρ^T at low temperatures. It is usual to assume[1-5] that in the range 1.5–4.5°K the resistivity rises with temperature approximately as T^2. The same dependence is observed also in the range 5–17°K but the coefficient of proportionality is different. Various explanations of the nature of this dependence have been proposed.

Gantmakher and Leonov[2] drew attention to the fact that the dependence $\rho \propto T^2$ may be due to the electron-phonon scattering if the constant-energy surface is a cylinder. Since in the case of bismuth the constant-energy surfaces of electrons can be regarded approximately as strongly elongated ellipsoids, Gantmakher and Leonov suggested that these dependences are due to the electron-phonon scattering in bismuth and, therefore, the resistivity of bismuth at $T < 4.2°$K is—in their opinion—due to this type of scattering.

Cheremisin[6] calculated the average (over the angles) relaxation time of electrons interacting with phonons in bismuth, whereas Medvedev, Kopylov, and Mezhov-Deglin[7] determined the temperature dependences of the mean free paths of electrons and holes relative to scattering by phonons at $T > 1°$K. The results obtained in Refs. 6 and 7 were in qualitative agreement with the experimental data from Ref. 8, according to which the dependence of the resistivity on T in the range 1.3–7°K is best described by $\rho^T = bT^{1.6 \pm 0.1}$. On the other hand, the quadratic temperature dependence of the resistivity was attributed in Refs. 5, 9, and 10 to the electron-hole scattering.

The problem became much clearer when Uher and Pratt[11] determined the resistivity of bismuth for five samples at infralow temperatures down to $T = 0.03°$K. Their results showed that at sufficiently low temperatures the resistivity decreases faster than quadratically

with decrease in temperature and that it is impossible to describe the temperature dependence of ρ^T throughout the range $0.03 < T < 4°$K by a power law. Consequently, the resistivity is not due to the electron-hole scattering, but most probably due to the intravalley scattering of carriers by phonons. However, the attempt of Uher and Pratt[11] to describe their dependences using the Bloch-Grüneisen formula for the phonon resistivity was only partly successful. They used two adjustable parameters and obtained agreement with the experimental results for a polycrystalline sample at $T < 1°$K. However, a good agreement was not obtained for single crystals.

Kukkonen[12] tried to explain the results of Uher and Pratt[11] by approximating the electron ellipsoids with cylinders of finite length (the phonon spectrum and the electron-phonon interaction were assumed to be isotropic). He used two adjustable parameters and achieved a good agreement with the results of Uher and Pratt[11] for two samples at $T > 0.5°$K.

However, there is no need to adopt these simplifications since the parameters of the electron, hole, and phonon spectra, as well as the deformation potential constants of bismuth are well known, so that the tensor describing the resistivity of bismuth due to the intravalley scattering by phonons can be calculated in a much more realistic approximation than those adopted earlier.

Such a calculation is reported below. We determined the phonon resistivity of electrons and holes in the range 0.1–8°K. This allowed us to dispense with the adjustable parameters and still obtain a satisfactory agreement with the experimental results of Uher and Pratt[11] in a wide temperature range 0.15–4°K where the resistivity changed by almost four orders of magnitude. We also found that the model of cylindrical constant-energy surfaces[2] describes bismuth poorly and the quadratic temperature dependence of the resistivity which follows from this model applies only in a very narrow temperature range.

1. MODELS OF ELECTRON, HOLE, AND PHONON SPECTRA

The Fermi surfaces of electrons and holes in bismuth are well known.[13] The electron surfaces are three quasi-ellipsoids, which transform into one another on rotation by 120° about the trigonal (Z) axis of the crystal. One of the quasiellipsoid axes coincides with the binary (X) axis of the crystal, whereas the other two axes are rotated by an angle $\eta \approx 6°$ relative to the crystallographic axes. The experimentally determined volume of the electron surface is $V_e = 14.66 \times 10^{-63}$ g^3 · cm^3 · sec^{-3}, which corresponds to an electron density $n = 3.02 \times 10^{17}$ cm^{-3}. Sections of the electron surface by planes perpendicular to the major (2) axis of the quasiellipsoid are very nearly ellipses.[13,14] The sections perpendicular to the other axes differ slightly from the elliptical shape. However, as shown in Ref. 13, the electron Fermi surface of bismuth can be described (with an average rms error of 1.26%) by the following ellipsoid:

$$\frac{p_1^2}{p_{10}^2} + \frac{p_2^2}{p_{20}^2} + \frac{p_3^2}{p_{30}^2} = 1, \tag{1}$$

where $p_{10} = 0.564 \times 10^{-21}$, $p_{20} = 8.405 \times 10^{-21}$, and $p_{30} = 0.743 \times 10^{-21}$ g · cm · sec^{-1}.

The electron spectrum is strongly nonparabolic. It is at present assumed that among the relatively simple models of the electron spectrum is bismuth, the best description of the electron surface is given by the Cohen model.[13] In this model the tensors of the effective masses on the Fermi surface depend on the position of a given point. However, since a consistent calculation of the electrical conductivity allowing for the anisotropy of the spectrum of the particles and phonons can be made only in the case of ellipsoidal constant-energy surfaces and since the electrical conductivity of a degenerate electron gas is governed (in the case of ellipsoidal constant-energy surfaces) by the masses on the Fermi surface, we shall approximate the electron spectrum by

$$\varepsilon = \frac{p_1^2}{2m_1} + \frac{p_2^2}{2m_2} + \frac{p_3^2}{2m_3}, \tag{2}$$

where m_i are the masses on the Fermi surface (the nonparabolicity is allowed for in the values of the masses). We shall assume that the masses m_i have the values given in Ref. 15:

$$m_1 = 0.00597 m_0; \quad m_2 = 1.33 m_0; \quad m_3 = 0.0114 m_0.$$

Naturally, for this electron spectrum we can expect a significant error in the calculation of σ_{22}, but since m_2 is large compared with m_1 and m_3, the value of σ_{22} is small and this introduces no significant error in the total electrical conductivity.

In contrast to the electron spectrum, the hole spectrum is parabolic. The constant-energy surface is then an ellipsoid whose revolution axis coincides with a crystallographic axis. The hole masses are $M_\parallel = 0.69 m_0$, $M_\perp = 0.064 m_0$. The phonon spectrum for bismuth can be taken from Ref. 16.[1)]

2. ELECTRICAL CONDUCTIVITY TENSOR

The matrix elements of the interaction between elec-

trons and phonons are

$$W_{\mathbf{p},\mathbf{p-q}}^{(\alpha)} = \frac{\pi}{4\rho V} \frac{1}{\omega^{(\alpha)}(\mathbf{q})} \left[\sum_{i,j} D_{i,j}^{e,h} (q_j e_i^{(\alpha)} + q_i e_j^{(\alpha)}) \right]^2. \tag{3}$$

Here, V is the volume of the crystal and $D_{i,j}^{e,h}$ are the tensors of the deformation potential constant for electrons and holes. The published[17-19] experimental values of these constants are consistent. We shall use the constants from Ref. 18:

$$D_{xx}^e = -2.2; \quad D_{YY}^e = 5.9; \quad D_{ZZ}^e = -1.7; \quad D_{YZ}^e = 1.5;$$
$$D_{xx}^h = D_{YY}^h \equiv D_\perp = 1.2; \quad D_{ZZ}^h \equiv D_\parallel = -1.2 \quad \text{eV}.$$

The transport equations for electrons and holes were solved by the variational method in the one-moment approximation. We shall omit the cumbersome intermediate stages (similar calculations were reported in Ref. 20 for an ellipsoid of revolution) and give only the final expressions for the electrical conductivity due to electrons and holes.

a) Electrons

The diagonal (in terms of the mass ellipsoid axes) components of the tensor representing the electrical conductivity due to electrons belonging to one quasi-ellipsoid can be described, with an accuracy to within terms of the order of $\sin^2 \eta \sim 10^{-2}$, by

$$\sigma_{ii}^e = n e^2 \tau_{ii}^e / m_i, \tag{4}$$

where

$$\tau_{ii}^e = \frac{16 \rho \pi^4 \hbar^7 m_3 n}{(k_0 T)^5 m_1 m_2 F_{ii}} \tag{5}$$

are the "effective relaxation times," and

$$F_{ii} = \sum_\alpha \int d\Omega_f f_i^2 \Lambda_e^{(\alpha)} (\mathbf{f}) c_\alpha^{-5}(\mathbf{f}) I_5(\Theta^{(\alpha)}(\mathbf{f})/T). \tag{6}$$

Here, $\mathbf{f}$ is a unit vector in the direction of the phonon quasimomentum. The quantities $c_\alpha(\mathbf{f})$ represent the phonon velocities in a "deformed" coordinate system in which a constant-energy ellipsoid transforms into a sphere. The quantity $\Lambda_e^{(\alpha)}(\mathbf{f})$ describes the angular dependence of the matrix element of the electron-phonon interaction in terms of these "deformed" coordinates. The function $I_5[\Theta^{(\alpha)}(\mathbf{f})/T]$ represents generalization of the Bloch integral:

$$I_5 \left(\frac{\Theta^{(\alpha)}(\mathbf{f})}{T} \right) = \int_0^{\Theta^{(\alpha)}(\mathbf{f})/T} \frac{z^5 e^z}{(e^z - 1)^2} dz, \tag{7}$$

$$\Theta^{(\alpha)}(\mathbf{f}) = 2 c_\alpha(\mathbf{f}) p_{30} / k_0. \tag{8}$$

Ignoring the angular dependence of the phonon velocity, we can obtain the following values of the minimum and maximum characteristic temperatures $\Theta^{(\alpha)}$ (Table I).

In the case of an prolate ellipsoid the function I_5 depends considerably on the angles and, in the final analysis, this alters greatly the temperature dependence of the electrical conductivity compared with that expected for an isotropic spectrum. If the spectra of electrons and phonons are isotropic, Eqs. (4)–(8) yield the usual expression for the low-temperature electrical conductivity of a degenerate electron gas.

The total electrical conductivity due to electrons is

TABLE I.

Θ	α	
	2	1,3
$\Theta_{min}^{(\alpha)}$	2.4	1.2
$\Theta_{max}^{(\alpha)}$	31.0	16.0

found by summing over the ellipsoids:

$$\Sigma_{XX}=\Sigma_{YY}=3(\sigma_{11}\textdegree+\sigma_{22}\textdegree)/2, \quad \Sigma_{ZZ}=3\sigma_{33}\textdegree. \tag{9}$$

Here, X, Y, and Z are the crystallographic axes.

In general, Σ_{XX} and Σ_{ZZ} include terms proportional to the nondiagonal (in terms of the mass ellipsoid axes) component of the electrical conductivity tensor, which differs from zero because the ellipsoid axes are rotated relative to the crystallographic axes. However, the contribution of the corresponding term in Σ_{ii} is proportional to $\sin^2 \eta$. Therefore, we shall omit it together with other terms proportional to $\sin^2 \eta$.

b) Holes

In this case we have

$$\sigma_{\perp,\parallel}^{h}=ne^2\tau_{\perp,\parallel}^{h}/M_{\perp,\parallel}, \tag{10}$$

$$\tau_{\perp,\parallel}^{h}=16\rho\pi^4\hbar^7 M_{\parallel}n/(k_0 T)^5 M_{\perp}^2 \Phi_{\perp,\parallel}, \tag{11}$$

$$\Phi_{\perp,\parallel}=\sum_{\alpha=2,3}\int d\Omega_f f_{\perp,\parallel}^2 s_\alpha^{-5}(\mathbf{f})\Lambda_h^{\alpha)}(\mathbf{f})I_5\left(\frac{\Theta^{(\alpha)}(\mathbf{f})}{T}\right). \tag{12}$$

Holes do not interact with a polarization wave 1. The quantities $\Lambda_h^{(\alpha)}(\mathbf{f})$ and $s_\alpha(\mathbf{f})$ have the same meaning as $\Lambda_e^{\alpha}(\mathbf{f})$ and $c_\alpha(\mathbf{f})$, and we also have

$$\Theta^{(\alpha)}(\mathbf{f})=2s_\alpha(\mathbf{f})p_{30}^{h}/k_0. \tag{13}$$

Table II gives the minimum and maximum values of $\Theta^{(\sigma)}$ for holes.

3. RESULTS OF NUMERICAL CALCULATIONS. COMPARISON WITH THE EXPERIMENTAL DATA

The electrical conductivities of electrons and holes were calculated using Eqs. (4)–(13) for the range 0.1–8°K using the parameters in Secs. 1 and 2.

Figure 1 shows the temperature dependences of the electrical conductivities of electrons and holes along a threefold axis and in the basal plane.

It follows from Eqs. (4)–(8) that at low temperatures such that $T \ll \Theta_{min}$, the electron conductivity reaches the low-temperature asymptote $\sigma^e \propto T^{-5}$. It is clear from Fig. 1 that this asymptote applies at $T < 0.15°K$. It follows from the same formulas (4)–(8) that in the temperature range $T \gg \Theta_{max}^{(\alpha)}$ the high-temperature asymptote $\sigma^e \propto T^{-1}$ begins to apply and—according to Fig. 1—this occurs at temperatures $T > 6°K$. Thus, the inter-

TABLE II.

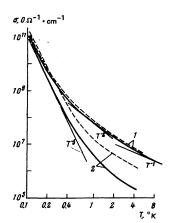| Θ	α	
	2	3
$\Theta_{min}^{(\alpha)}$	2.7	5.4
$\Theta_{max}^{(\alpha)}$	9.0	18.0

FIG. 1. Temperature dependences of the electron (1) and hole (2) electrical conductivities. The continuous curves represent the conductivity along the axis of a crystal and the dashed curves the conductivities at right-angles to the axis. The straight lines represent the power-law dependences identified in the figure.

mediate range corresponds to a change in temperature by a factor exceeding 40. For comparison, we shall mention that in the case of an isotropic metal this intermediate range is much narrower. It corresponds to a change in temperature by a factor of 8–10 (Ref. 21). Strictly speaking, the electron conductivity falls on increase in T faster than T^{-1} right up to the maximum characteristic temperature of Eq. (8), which—according to Table I—is $\Theta_{max}^{(3)}=31°K$. However, in practice the conductivity contribution of electrons with large momenta which are scattered through small angles becomes unimportant at much lower temperatures.

It is impossible to find a reasonably wide temperature range in which the conductivity would vary in accordance with the power law. It is clear from Fig. 1 that this applies also to the dependence $\sigma^e \propto T^{-2}$, which—according to Gantmakher and Leonov[2]— should be obeyed by bismuth. It is shown in the Appendix that this dependence holds only at temperatures satisfying a strong dipole inequality $\Theta_{min} \ll T \ll \Theta_{max}$. However, even in the case of a strongly prolate electron ellipsoid of bismuth the ratio of the characteristic temperatures is $\Theta_{max}^{(\alpha)}/\Theta_{min}^{(\alpha)} \approx 13$, so that the above inequality cannot be satisfied too well. The existence of two characteristic temperatures Θ_{min} and Θ_{max} has only the effect that the transition between the high- and low-temperature asymptotes is extended over a much wider range than in the isotropic case.

At the lowest temperatures the hole conductivity does not differ greatly from the electron conductivity. However, since the minimum characteristic temperature of holes $\Theta_{min}^{(\alpha)}=2.4°K$ is greater than the minimum temperature of electrons $\Theta_{min}^{(\alpha)}=1.2°K$, it follows that σ^h decreases with temperature faster than σ^e and right up to $T \approx 0.4°K$ the hole conductivity obeys $\sigma^h \propto T^{-5}$. Therefore, at $T > 1°K$ the contribution of holes to the conductivity of a crystal is less than 20%.

Figure 2 shows the temperature dependence of the conductivity anisotropy for one electron ellipsoid. In accordance with the qualitative results obtained in the
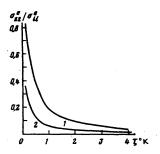
FIG. 2. Temperature dependences of $\sigma_{22}^e/\sigma_{ii}^e$: 1) $\sigma_{22}^e/\sigma_{33}^e$; 2) $\sigma_{22}^e/\sigma_{11}^e$.

Appendix, at low temperatures the ratios σ_{22}/σ_{11} and σ_{22}/σ_{33} are of the order of unity, but at higher temperatures these ratios decrease rapidly and at $T \approx 4-6°K$ they are of the order of m_{ii}/m_{22}.

We shall now compare our results with the experimental data. We must bear in mind that at low temperatures the carriers are scattered mainly by defects. According to the Matthiessen rule, the resistivity for the s-th group of carriers is

$$r_{ii}^{(s)} = (\sigma_{ii}^{(s)})^{-1} + (\bar\sigma_{ii}^{(s)})^{-1}, \tag{14}$$

where $(\sigma_{ii})^{-1}$ and $(\bar\sigma_{ii})^{-1}$ are, respectively, the diagonal components of the phonon and residual resistivities. We recall that the nondiagonal components are proportional to $\sin^2\eta$ and, therefore, can be omitted.

If we calculate the conductivity for each group, sum over all the groups (three electron ellipsoids and one hole ellipsoid), and calculate the residual resistivity which is

$$\left\{ \sum_{s=1}^{4} \bar\sigma_{ii}^{(s)} \right\}^{-1}, \tag{d}$$

we obtain the temperature-dependent part of the resistivity ρ^T:

$$\rho_{ii}^T$$

$$= \rho_{ii} - (\rho_{ii})_{0CT} = \left\{ \sum_{s=1}^{4} \frac{\sigma_{ii}^{(s)} \bar\sigma_{ii}^{(s)}}{\sigma_{ii}^{(s)} + \bar\sigma_{ii}^{(s)}} \right\}^{-1}$$

$$-\left\{ \sum_{s=1}^{4} \bar\sigma_{ii}^{(s)} \right\}^{-1}. \tag{15}$$

Since the residual resistivity of holes is considerably greater than that of electrons (according to the experimental data of Ref. 22 the scattering of holes by impurities is at least 15 times stronger than the scattering of electrons), we can ignore the contribution of holes to Eq. (15). Moreover, since $m_2 \gg m_1, m_3$, we can expect that $\bar\sigma_{22} \ll \bar\sigma_{11}, \bar\sigma_{33}$, and we can also ignore the contribution of the corresponding component of the conductivity. Finally, we find from Eq. (15) that

$$\rho_{zz}^T = (\sigma_{33}^e)^{-1}/3, \quad \rho_{xx}^T = 2(\sigma_{11}^e)^{-1}/3. \tag{16}$$

The resistivities ρ_{zz}^T and ρ_{xx}^T are those quantities which we shall compare with the experimental data.
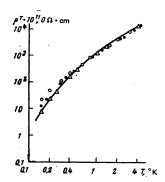
The temperature dependence of the total resistivity

FIG. 3. Temperature dependences of the transverse resistivity. The continuous curve is theoretical and the symbols are the experimental results: O) sample No. 2 ($\vartheta = 90°$); sample ●) sample No. 5 ($\vartheta = 79°$); △) sample No. 1 ($\vartheta = 85^*$).

of a crystal ρ_{XX}^T is shown in Fig. 3. This figure includes also the experimental results from Ref. 11 obtained[2] at $T \geqslant 0.15°K$ for sample No.2 oriented at an angle $\vartheta = 90°$ to the trigonal axis of the crystal, and for samples Nos. 1 ($\vartheta = 85°$) and 5 ($\vartheta = 79°$). In view of the slight difference between the orientations of these samples, the phonon resistivities should be practically the same. However, the experimental results for sample No. 2 differ from those for samples Nos. 1 and 5 at $T < 0.4°K$. The resistivity of sample No. 2 decreases with decrease in temperature much more slowly than the resistivity of samples Nos. 1 and 5. Since the resistivities of the latter two samples are identical in the range $T > 0.25°K$ and differ only slightly at $T < 0.25°K$, it is reasonable to compare the theory with the experimental results for these two samples. We can see that the theory (the theoretical curves are identical for all three samples) agrees well with the experimental results throughout the range $4 > T > 0.15°K$.

Figure 4 shows the theoretical and experimental results for example No. 3 oriented at an angle $\vartheta = 49°$ to the trigonal axis. The agreement between the theory and experiment is fully satisfactory at $T < 4°K$.

Figure 5 gives the theoretical and experimental results for a polycrystalline sample. In this case the theory agrees satisfactorily with the experimental results only in the range $0.6 < T < 5°K$. At lower temperatures the

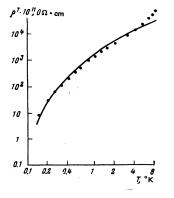
FIG. 4. Temperature dependence of the resistivity of sample No. 3 ($\vartheta = 49°$). The continuous curve is theoretical and the points are the experimental values.
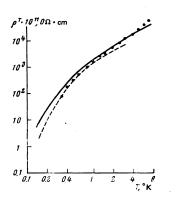
FIG. 5. Temperature dependence of the resistivity of a poly-crystalline sample. The continuous curve is theoretical, the points are the experimental values, and the dashed curve is calculated on the basis of the Bloch–Grüneisen formula with the parameters from Ref. 11.

experimental resistivity falls with decrease in temperature faster than the theoretical value. However, at low temperatures the experimental results for a polycrystalline sample disagree not only with the theory but also with the data for sample No. 3. Since the resistivity anisotropy of this crystal is slight, the phonon resistivities of the polycrystalline sample and of sample No. 3 should be almost identical. However, a comparison of Figs. 4 and 5 shows that in the range $T < 0.4°K$ the resistivity of a polycrystalline sample is considerably less than the resistivity of sample No. 3.

It is natural to assume that the phonon component of the resistivity can be identified much more reliably for a single crystal than for a polycrystalline sample, so that the discrepancy between the theory and experiment at ultralow temperatures observed for sample No. 4 is mainly due to the fact that the phonon resistivity of the polycrystalline sample is not separated sufficiently reliably.

The following comments can be made in this connection. If, using the adjustable parameters from Ref. 11, we calculate the resistivity using the Bloch-Grüneisen formula, we obtain the dashed curve shown in Fig. 5. The intermediate range of temperatures on this curve is, as expected, narrower than for the continuous curve and the asymptote $\rho^T \propto T^5$ begins at higher temperatures. This is why the isotropic model can describe satisfactorily the results of Ref. 11 for polycrystalline samples at $T < 1°K$.

Unfortunately, it is not possible to determine reliably the resistivity anisotropy from the experimental results because of the lack of measurements of ρ_{XX}^T and ρ_{ZZ}^T on the same sample, and the results obtained for different samples disagree. Nevertheless, an analysis of the experimental angular dependence of the resistivity leads to the conclusion that the ratio $(\rho_{ZZ}^T / \rho_{XX}^T)_{exp}$ depends weakly on temperature and varies within the range 1–1.3. The theoretical ratio lies within the range 1.1–1.2.

It is clear from Figs. 4 and 5 that at temperatures $T > 4°K$ the resistivity due to the intravalley scattering of electrons rises with temperature much more slowly than the experimental value. We may assume that the

intervalley scattering of electrons and holes begin to play a role in the same temperature range.

4. CONCLUSIONS

It is clear from the analysis given in the preceding section that the resistivity of bismuth due to the intravalley scattering of carriers by phonons may be calculated with an accuracy sufficient to ensure a good quantitative agreement with the experimental results in a wide range of low temperatures $0.15 < T < 4°K$. In the range $0.4 < T < 4°K$ the agreement is good for all the samples, whereas at temperatures $0.15 < T < 0.4°K$ it is good for three out of five samples investigated in Ref. 11.

The fact that the experimental data for the phonon resistivity of samples of almost the same orientation differ very strongly from one another also at $T < 0.4°K$ shows that the separation of the phonon component of the resistivity from the total value given in Ref. 11 is not fully reliable and this may be due to the presence of dislocations in the samples. In our opinion, this is one of the main reasons why the theory and experiment do not always agree at ultralow temperatures.

The remaining discrepancies may also be due to simplifications made by us in the models of the electron and phonon spectra. Refinement of these models may alter somewhat the whole temperature dependence of the resistivity in the intermediate range of temperatures.

Finally, we recall that the Matthiessen rule for the total resistivity of bismuth is obeyed, as indicated by Eqs. (15) and (16), only approximately even in the absence of dislocations. However, it is at present impossible to apply directly Eq. (15) to calculate ρ^T because this requires the knowledge of the total residual resistivity tensors of electrons and holes. It would be highly desirable to determine experimentally these tensors.

APPENDIX

We shall consider qualitatively the temperature dependence of the electrical conductivity tensor for one ellipsoid using the following simplified model. Firstly, we shall assume that the phonon spectrum is isotropic. Secondly, we shall replace a triaxial electron ellipsoid with an ellipsoid of revolution characterized by $m_\perp \approx \sqrt{m_1 m_3}$, $m_\parallel = m_1$; $p_{\perp 0} = \sqrt{p_{10} p_{30}}$, $p_{\parallel 0} = p_{20}$. Finally, we shall assume that $D_\perp \approx \sqrt{D_{11} D_{33}}$, $D_\parallel = D_{22}$. In this approximation the electron resistivity due to the scattering by longitudinal phonons is

$$\rho_\parallel' = 2A_l T^5 \frac{m_\parallel}{m_\perp} \int_0^\pi d\vartheta \sin \vartheta \cos^2 \vartheta \frac{(\alpha \sin^2 \vartheta + \cos^2 \vartheta)^2}{(\beta \sin^2 \vartheta + \cos^2 \vartheta)^4} I_5 \left(\frac{\Theta'(\vartheta)}{T} \right) \Bigg\} \quad (A1)$$

$$\rho_\perp' = A_l T^5 \int_0^\pi d\vartheta \sin^3 \vartheta \frac{(\alpha \sin^2 \vartheta + \cos^2 \vartheta)^2}{(\beta \sin^2 \vartheta + \cos^2 \vartheta)^4} I_5 \left(\frac{\Theta'(\vartheta)}{T} \right),$$

$$k_0 \Theta' = 2 p_{\parallel 0} s_l^0 (\beta \sin^2 \vartheta + \cos^2 \vartheta)^{1/2}, \quad (A2)$$

$$s_i{}^\circ = \left(\frac{c_{11}}{\rho}\right)^{1/2}, \quad \beta = \frac{p_{\perp 0}{}^2}{p_{\parallel 0}{}^2} = \frac{m_\perp}{m_\parallel} \ll 1, \quad \alpha = \frac{D_\perp}{D_\parallel}\beta \ll 1. \tag{A3}$$

The constant obeys $A_i \propto D_\parallel^2$.

At high temperatures defined by

$$k_0 T \gg k_0 \Theta_{max} = 2p_{\parallel 0}s_i{}^\circ$$

the integral is

$$I_5(\Theta^i(\vartheta)/T) \sim (\Theta^i(\vartheta)/T)^4$$

and the resistivity obeys $\rho_{\parallel,\perp}^i \propto T$.

In this case the numerators and denominators of the resultant integrands can be simplified by dropping the terms proportional to α and β, because the integrals in Eqs. (A1) and (A2) are of the same order of magnitude, i.e., the resistance anisotropy is $\rho_\parallel/\rho_\perp \sim m_\parallel/m_\perp \gg 1$, and the scattering anisotropy is weak. The weakness of the scattering anisotropy is associated with the fact that at high temperatures all electrons are scattered through large angles irrespective of the direction of their momentum.

At low temperatures defined by $k_0 T \ll k_0 \Theta_{min} \equiv 2p_{\perp 0}s_i$ we have $I_5 = \text{const}$ and the resistivity obeys $\rho \propto T^5$.

The integrands in Eqs. (A1) and (A2) have a sharp maximum at $\cos\vartheta \sim \beta$, so that the integral (A1) is $m_\parallel/m_\perp$ times less than the integral (A2). In other words, $\rho_\parallel^i$ and $\rho_\perp^i$ are of the same order of magnitude and the scattering anisotropy is of the order of the mass anisotropy. The strong scattering anisotropy at low temperatures is explained by the fact that all electrons are scattered by phonons whose momentum is $q \sim k_0 T/s$. In the case of electrons with high values of p, which move along the ellipsoid axis, this scattering is less effective than for electrons with small values of p moving across the axis.

We shall now consider the intermediate temperature range

$$2p_{\perp 0}s_i{}^\circ \ll k_0 T \ll 2p_{\parallel 0}s_i{}^\circ. \tag{A4}$$

We can easily see that in this case again we can simplify the integrands by dropping the terms containing α and β, so that Eqs. (A1) and (A2) transform to

$$\left.\begin{array}{l} \rho_\parallel{}' = 2A_i T^5 \dfrac{m_\parallel}{m_\perp} \displaystyle\int_0^1 \dfrac{dx}{x^2} I_5\left(\dfrac{\Theta_{max}x}{T}\right), \\[4mm] \rho_\perp{}' = 2A_i T^5 \displaystyle\int_0^1 \dfrac{dx}{x^4} I_5\left(\dfrac{\Theta_{max}x}{T}\right). \end{array}\right\} \tag{A5}$$

If $x > T/\Theta_{max} \ll 1$, the integrands decrease rapidly on increase in x. Therefore, the upper limits in these integrals should be replaced with infinity and then, introducing the variable $y = \Theta_{max}x/T$, we obtain

$$\rho_\parallel{}' = 2A_i \Theta_{max} \frac{m_\parallel}{m_\perp} T^4 \int_0^\infty \frac{dy}{y^2} I_5(y),$$

$$\rho_\perp{}' = 2A_i \Theta_{max}^3 T^2 \int_0^\infty \frac{dy}{y^4} I_5(y). \tag{A6}$$

The ratio of these resistivities is

$$\rho_\parallel{}'/\rho_\perp{}' \approx (T/\Theta_{min})^2 \gg 1. \tag{A7}$$

At the ends of the range defined by Eq. (A4) we find that Eq. (A7) gives the high-temperature ($\rho_\parallel^i/\rho_\perp^i \sim m_\parallel/m_\perp$) and low-temperature ($\rho_\parallel^i/\rho_\perp^i \sim 1$) asymptotes.

We can show that the resistivity ρ^t due to the scattering by transverse phonons is of the order of ρ^l at temperatures $T \ll \Theta_{min}$, but is less than ρ^l by a factor T/Θ_{max} in the range $\Theta_{min} \ll T \ll \Theta_{max}$ and by a factor $m_\parallel/m_\perp$ in the range $T \gg \Theta_{max}$.

---

[1] The expression for $e_z^{(2)}$ in Ref. 16 should be replaced with $e_z^{(2)} = -qz/\varkappa$.

[2] In Ref. 11 the measurements were carried out only down to $T = 0.03°K$ but in the range $T < 0.15°K$ the temperature-dependent part of the resistivity became very small and could not be separated from the total resistivity.

[1] A. N. Friedman, Phys. Rev. 159, 553 (1967).
[2] V. F. Gantmakher and Yu. S. Leonov, Pis'ma Zh. Eksp. Teor. Fiz. 8, 264 (1968) [JETP Lett. 8, 162 (1968)].
[3] V. Chopra, R. K. Ray, and S. M. Bhagat, Phys. Status Solidi A 4, 205 (1971).
[4] C. A. Kukkonen and K. F. Sohn, J. Phys. F 7, L193 (1977).
[5] E. W. Fenton, J.-P. Jan, A. Karlsson, and R. Singer, Phys. Rev. 184, 663 (1969).
[6] S. M. Cheremisin, Zh. Eksp. Teor. Fiz. 65, 1564 (1973) [Sov. Phys. JETP 38, 779 (1974)].
[7] E. S. Medvedev, V. N. Kopylov, and L. P. Mezhov-Deglin, Fiz. Nizk. Temp. 1, 1192 (1975) [Sov. J. Low Temp. Phys. 1, 572 (1975)].
[8] V. N. Kopylov and L. P. Mezhov-Deglin, Zh. Eksp. Teor. Fiz. 65, 720 (1973) [Sov. Phys. JETP 38, 357 (1974)].
[9] R. Hartman, Phys. Rev. 181, 1070 (1969).
[10] C. A. Kukonen and P. F. Maldague, J. Phys. F 6, L301 (1976).
[11] C. Uher and W. P. Pratt Jr, Phys. Rev. Lett. 39, 491 (1977).
[12] C. A. Kukonen, Phys. Rev. B 18, 1849 (1978).
[13] V. S. Édel'man, Usp. Fiz. Nauk 123, 257 (1977) [Sov. Phys. Usp. 20, 819 (1977)].
[14] J. F. Koch and J. D. Jensen, Phys. Rev. 184, 643 (1969).
[15] R. J. Dinger and A. W. Lawson, Phys. Rev. B 7, 5215 (1973).
[16] I. Ya. Korenblit, Fiz. Tekh. Poluprovodn. 2, 1425 (1968) [Sov. Phys. Semicond. 2, 1192 (1969)].
[17] S. Inoue and M. Tsuji, J. Phys. Soc. Jpn. 22, 1191 (1967).
[18] K. Walther, Phys. Rev. 174, 782 (1968).
[19] T. Fukami, T. Yamaguchi, and S. Mase, J. Phys. Soc. Jpn. 47, 423 (1979).
[20] V. S. Vinnik, E. A. Okhrem, and A. G. Samoĭlovich, Fiz. Nizk. Temp. 4, 879 (1978) [Sov. J. Low Temp. Phys. 4, 417 (1978)].
[21] F. J. Blatt, Physics of Electronic Conduction in Solids, McGraw-Hill, New York, 1968 (Russ. Transl., Mir, Moscow, 1971), Chap. 7.
[22] J. P. Issi, J. P. Michenaud, and J. Heremans, Phys. Rev. B 14, 5156 (1976).

Translated by A. Tybulewicz

1062   Sov. Phys. JETP 53(5), May 1981

Vinnik et al.   1062